Enhanced Ultraviolet Emission from Poly(vinyl alcohol) ZnO Nanoparticles Using a SiO2−Au Core/Shell Structure

Article *in* Nano Letters · October 2012

Impact Factor: 13.59 · DOI: 10.1021/nl3031955 · Source: PubMed

5 authors, including:

Hongtao Sun
University of California, Los Angeles
36 PUBLICATIONS **933** CITATIONS

SEE PROFILE

Mingpeng Yu
Tsinghua University
39 PUBLICATIONS **729** CITATIONS

SEE PROFILE

NANO LETTERS

Letter

pubs.acs.org/NanoLett

Enhanced Ultraviolet Emission from Poly(vinyl alcohol) ZnO Nanoparticles Using a SiO_2–Au Core/Shell Structure

Dali Shao,*[,†] Hongtao Sun,[‡] Mingpeng Yu,[‡,§] Jie Lian,[‡] and Shayla Sawyer[†]

[†]Department of Electrical, Computer, and Systems Engineering and [‡]Department of Mechanical, Aerospace, and Nuclear Engineering, Rensselaer Polytechnic Institute, Troy, New York 12180, United States

[§]Department of Physics, School of Mathematics and Physics, University of Science and Technology Beijing, 30 Xueyuan Road, Haidian District, Beijing 100083, China

ABSTRACT: Enhanced near band gap edge (NBE) emissions of PVA–ZnO nanoparticles were achieved by employing SiO_2–Au core/shell nanostructures whereas the defect-level emission (DLE) is greatly suppressed. A maximum enhancement of nearly 400% was observed using SiO_2–Au for the emission with optical resonance at 554 nm. SiO_2–Au core/shell nanostructures also show a superior tunability of resonance energy as compared to that of the pure metal nanoparticles. The enhancement of the NBE emission and suppressed DLE is ascribed to the transfer of the energetic electrons excited by surface plasmon from metal nanoparticles to the conduction band of ZnO nanoparticles.

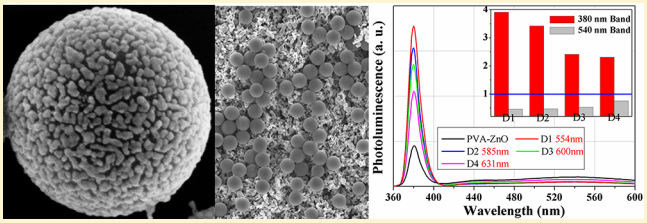

KEYWORDS: *SiO_2–Au core/shell, ZnO nanoparticles, photoluminescence, surface plasmon resonance*

Investigations of surface plasmon resonance (SPR) effects from metallic nanostructure/dielectric interfaces have increased in recent research because of their promising applications in the enhancement of the luminescence efficiency of light-emitting materials and devices.[1−5] Among direct band gap semiconductor materials, ZnO is considered to be one of the most promising materials for ultraviolet LEDs and laser diodes because of its large band gap (3.36 eV) and high exciton binding energy (60 meV). Enhanced UV emission of ZnO has been achieved by the deposition of metals such as Ag, Au, Al, and Pt on ZnO films, as a result of the resonant coupling between the surface plasmon of metal and the band gap emission of ZnO.[1−4] However, the tunability of the resonance of pure metal particles is limited. For example, by increasing the size of gold nanoparticles from 5 to 80 nm, the resonance peak can shift only from 520 to 545 nm.[6] Moreover, the synthesis of monodisperse metal nanoparticles with sizes larger than 100 nm is a significant challenge.[7,8] As a promising alternative, the resonance peak of colloidal metal core shell structures can be easily tuned over a wide range by changing the core-to-shell ratio. Therefore, colloidal core–shell metal nanoparticles greatly enhance the ability to manipulate the resonating conduction electrons, making it possible to cover the ultraviolet, visible, and infrared wavelengths of the electromagnetic spectrum.[9]

In this letter, we report enhanced UV emission by the deposition of solution-processed SiO_2–Au core shell nanostructures on the PVA–ZnO nanoparticle thin film surface. ZnO nanoparticles with sizes ranging from 100 to 150 nm were surface treated with PVA solutions (1% by weight of water) for surface passivation. The PVA-coated ZnO nanoparticles were then centrifuged and dispersed in ethanol to form a suspension with a concentration of 30 mg/mL. The solution was spin-coated onto quartz substrates and annealed in air at 100 °C for 5 min, followed by the deposition of SiO_2–Au core–shell nanoparticles through a simple drop-casting method.

An outline of the gold-functionalized silica particles is shown in Figure 1, which is a modified method described by Oldenburg et al.[10] and Westcott et al.[11] Silica spheres were first obtained using the Stöber procedure.[12] A solution of 30 mL of ammonia and 4 mL of tetraethoxysilane (TES) were added to 200 mL of dry ethanol under rapid stirring (>150 rpm). The functionalizations were carried out by mixing a certain amount of 3-aminopropyltrimethoxysilane (APS), which was sufficient to provide an approximately 2.5 monolayer coating on the silica particles. After it was stirred overnight, the solution was held at a low boil (80 °C) for 1 h to promote covalent bonding of the organosilane to the surface of the silica particles.[13,14] Excess reactants were removed from the APS-functionalized particles by centrifugation and redispersion in ethanol at least five times.

Aqueous solutions of small gold nanoclusters (1 to 2 nm in diameter) were prepared by the reduction of chloroauric acid with tetrakis hydroxymethyl phosphonium chloride (THCP) as described by Duff et al.[15] An appropriate amount of APS-functionalized silica particles was added dropwise to the freshly prepared gold nanocluster solution and stirred for 12 h in order to form silica particles covered with small gold clusters

Received: August 28, 2012
Revised: October 20, 2012
Published: October 24, 2012

   dx.doi.org/10.1021/nl3031955 | *Nano Lett.* 2012, 12, 5840−5844

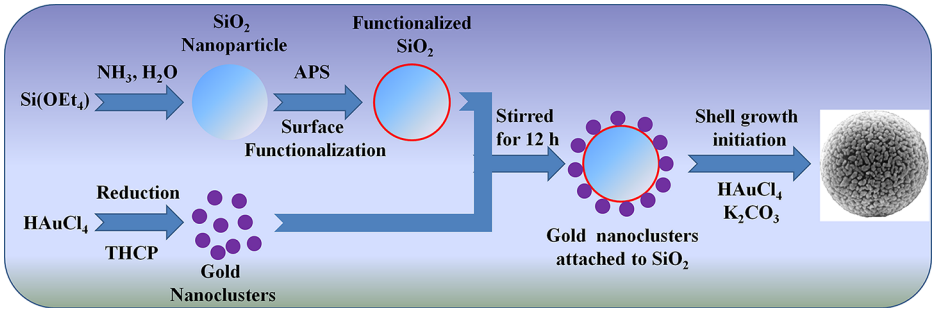

Figure 1. Scheme of the synthesis of the SiO_2–Au core–shell structures.

(precursor particles). Nonattached gold nanoclusters were removed by centrifugation and redispersion in water.

To initiate the growth of the gold shell, silica particles attached to gold nanoclusters were added to the aged mixture solution (gold hydroxide) of chloroauric acid and potassium carbonate.[16] The surface coverage or shell thickness can be easily controlled by adjusting the ratio of the number of precursor particles to the gold salt. These suspensions were centrifuged to remove excess reagents for further characterization.

The scanning electron microscope (SEM) images of SiO_2–Au core/shell samples (S1–S4) with varying dimensions (5–40 nm) of Au nanoparticles attached to the surface of SiO_2 are shown in Figure 2a–d. The dimensions of the SiO_2 core of samples S1–S4 are similar at about 600 nm. A larger-scale SEM image of the SiO_2–Au core–shell structure is presented in Figure 2e. An X-ray photoelectron spectroscopy (XPS) spectrum from 0 to 1000 eV for the SiO_2–Au core–shell structures is shown in Figure 3a, revealing the presence of Si, O, Au, and C. The C signal may originate from adventitious carbon contamination. Figure 3b shows the X-ray diffraction (XRD) pattern of the SiO_2–Au core–shell structures in which one weak diffraction peak can be indexed to SiO_2 in addition to peaks from gold shells.

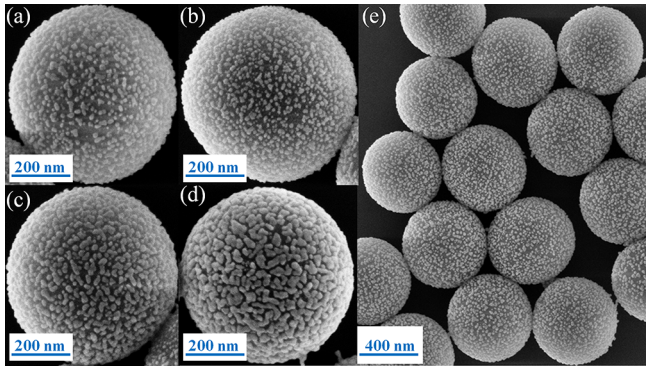

Figure 2. (a–d) High-resolution SEM images of the SiO_2–Au core–shell samples (S1–S4) with varying dimension of Au nanoparticles attached to the surface of SiO_2. (e) SEM image of a SiO_2–Au core–shell sample on a larger scale.

To test the tunability of the surface plasmon resonance coupling of the SiO_2–Au core–shell structures, samples S1–S4 are deposited on PVA-coated ZnO nanoparticle thin films by a drop casting method to form SiO_2–Au/PVA–ZnO composite structures, which are labeled as D1–D4. The planar and cross-sectional SEM images of the SiO_2–Au/PVA–ZnO composite structures are shown in Figure 4a–c, respectively. The ZnO nanoparticles have an average size ranging from 100 to 150 nm. The photoluminescence (PL) spectra of samples D1–D4 and the reference sample (bare PVA–ZnO without deposition of SiO_2–Au) were measured using a Spex Fluorolog Tau-3 spectrofluorimeter with a xenon lamp, and the excitation wavelength was fixed at 330 nm, as shown in Figure 5. The spectra consist of two bands at 380 and 540 nm, respectively. The first band is attributed to NBE emission, and the second band originates from deep defect levels induced by oxygen vacancies.[17–19] The enhancement factor is defined as the ratio of the intensity of the PL peak for the composite structure sample to that of the PL peak for the reference sample. The enhancement factors for NBE recombination (red pillar) and DLE (gray pillar) are presented in the inset of Figure 5. It is found that the enhancement factor of the NBE emission

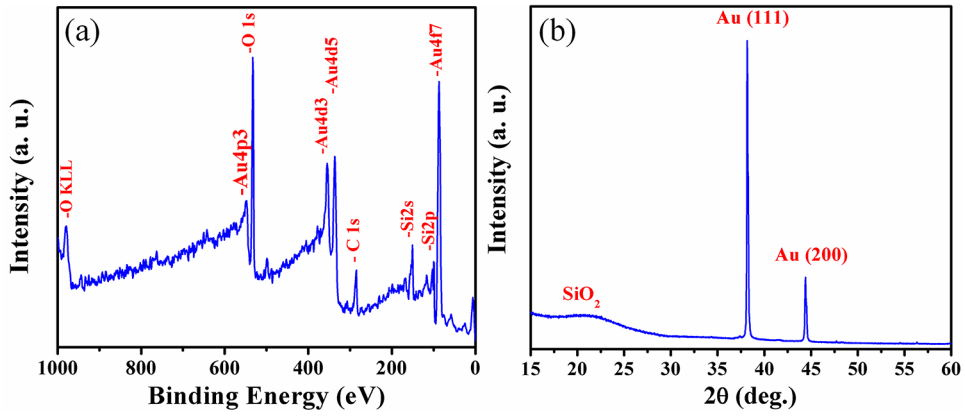

Figure 3. (a) XPS analysis and (b) XRD pattern of SiO_2–Au core–shell structures.

dx.doi.org/10.1021/nl3031955 | Nano Lett. 2012, 12, 5840–5844

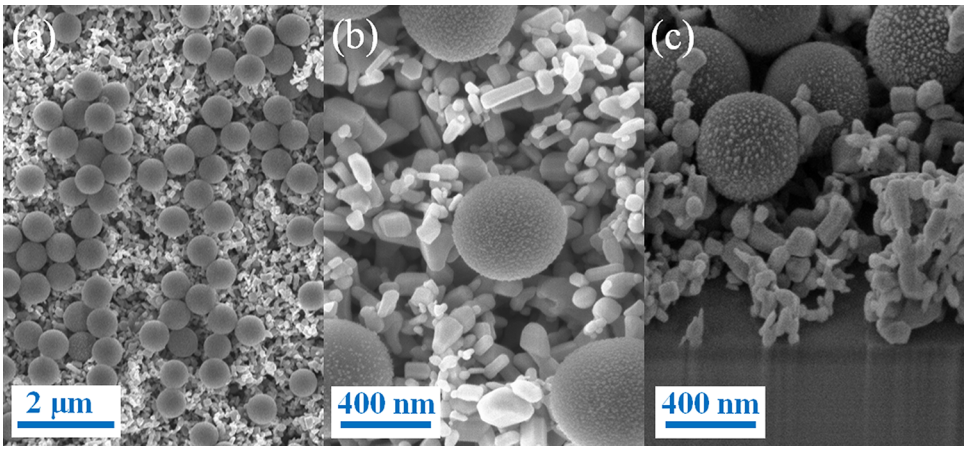

Figure 4. (a, b) Planar and (c) cross-sectional SEM images of the SiO_2−Au/PVA−ZnO composite structures.

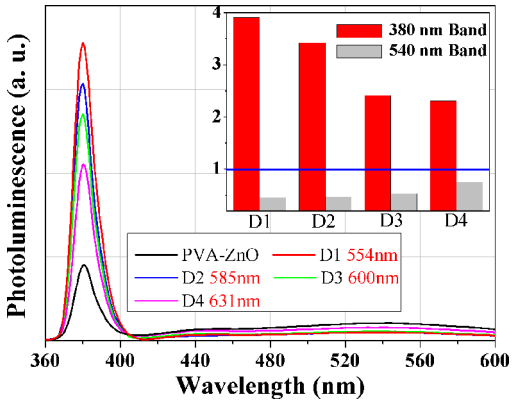

Figure 5. PL spectra of D1−D4 (with different resonance peaks) and reference sample (PVA−ZnO). The inset is the enhancement factor for band edge emission and defect-level emission from D1 to D4.

increases from sample D1 to D4 and the enhancement factor of the defect-related emission band decreases. The change in the PL enhancement factors for the 380 nm emission band and the 540 nm emission band of D1−D4 is attributed to the resonance effect between the surface plasmon of metal nanoparticles and defect emission, which converts the useless defect radiation to useful excitonic emissions. This mechanism is illustrated in Figure 6. The Au Fermi level is 5.3 eV below the vacuum level, which is very close to the energy defect level of ZnO (5.35 eV below the vacuum level). This enables the electron transfer from the ZnO defect levels to the Fermi level of Au, thus increasing the electron density in Au.[20] Upon resonance

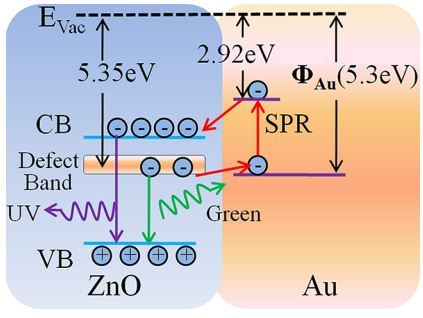

Figure 6. Scheme of the SPR effect of the Au shell on the suppression of the defect emission and the enhancement of the NBE emissions.

excitation, particle plasmons can undergo a nonradiative decay via excitation of electron−hole pairs and create energetic electrons with higher-energy states in Au.[21] The surface plasmon energy of Au is around 2.38 eV, making the created energetic electrons 2.92 eV below the vacuum level. These energetic electrons can be transmitted to the conduction band of ZnO.[22] Therefore, the electrons in defect states have a pathway to the conduction band of ZnO via Au, leading to an increase in the number of electrons in the conduction band of ZnO. Hence, the NBE emission is enhanced while the defect emission is reduced.

The proposed mechanism for PL enhancement is supported by the absorption spectra measurement, as shown in Figure 7.

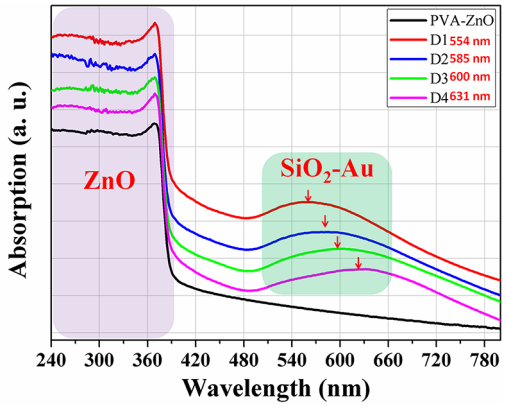

Figure 7. Absorption spectra of D1−D4 with resonance peaks ranging from 554 to 631 nm.

The absorption peak at about 380 nm is assigned to the intrinsic exciton absorption of the ZnO film, and the extra absorption peaks observed at 554, 585, 600, and 631 nm can be attributed to the surface plasmon resonance (SPR) absorption of SiO_2−Au core−shell structures deposited on top of samples D1−D4. Such SPR absorption was also reported for Ag nanoparticles implanted in ZnO films.[23] The position of the ZnO DLE is close to the SPR wavelength of SiO_2−Au core−shell structures, making it possible to couple between them resonantly. The maximum PL enhancement observed for sample D1 can be explained by its closer proximity to the ZnO DLE wavelength (540 nm) than samples D2, D3, and D4. Hence, D1 has the largest enhancement factor. It is clear from Figure 7 that by varying the dimension of the Au nanoparticles

dx.doi.org/10.1021/nl3031955 | Nano Lett. 2012, 12, 5840−5844

attached to the SiO_2 surface from 5 to 40 nm the core−shell structures show tunable resonance peaks that can shift from 554−631 nm (77 nm difference). This proves the superior tunability of the SiO_2−Au core−shell structure as compared to that of pure Au nanoparticles.

To investigate the SPR mechanism of the composite material system further, time-resolved PL (TRPL) measurements were carried out under excitation by the fourth harmonic (266 nm) of the mode-locked Nd^{3+}/YAG laser with a pulse duration of 20 ps. The TRPL signal was recorded using a streak camera with 2 ps temporal resolution, and the result is shown in Figure 8. The

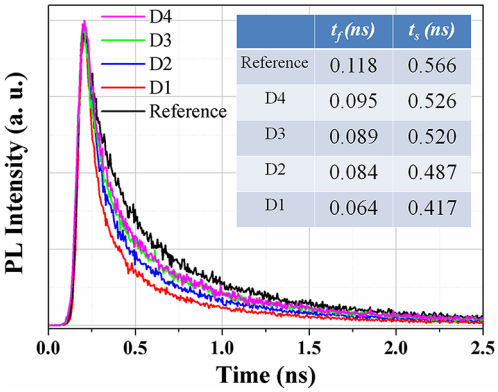

	t_f (ns)	t_s (ns)
Reference	0.118	0.566
D4	0.095	0.526
D3	0.089	0.520
D2	0.084	0.487
D1	0.064	0.417

Figure 8. TRPL decay transients measured for D1−D4 and the reference sample.

decay trace can be approximately fitted by a biexponential function as follows: $y = y_0 + A_s \exp[-(t - t_0)/t_f] + A_f \exp[-(t - t_0)/t_s]$. In the fitting equations, y_0, t_0, A_f, and A_s are the fitting parameters, and t_f and t_s are fast and slow exciton decay times. The value of t_f and t_s for each sample is listed in the inset of Figure 8, which shows that the lifetimes of the exciton transition from the samples with SiO_2−Au core−shell structures are faster than that from bare PVA−ZnO. This observation provides further evidence of the proposed SPR mechanism.

In conclusion, SiO_2−Au core−shell structures with a controllable core−shell ratio were synthesized, and the SPR peaks of the core−shell structures can be tuned over a wide range (554−631 nm) by adjusting the size and the shape of Au nanoparticles attached to the SiO_2 surface. The core−shell structures provide an effective approach for simultaneously suppressing DLE and enhancing NBE emissions of the ZnO nanoparticles by defect-induced surface plasmon resonance. The superior SPR tunability of the core−shell structure, together with the low cost and flexibility of the approach, makes it a nanomaterial of high potential for future optoelectronics. Future work will focus on investigating methods to pattern the SiO_2−Au core−shell structures precisely and the influence of SPR tunability in further improving the PL enhancement.

AUTHOR INFORMATION

Notes

The authors declare no competing financial interest.

ACKNOWLEDGMENTS

We gratefully acknowledge support from the National Security Technologies through NSF Industry/University Cooperative Research Center Connection One. We also acknowledge the National Science Foundation Smart Lighting Engineering Research Center (EEC-0812056) and NSF career award DMR 1151028. M.Y. is grateful for financial support from the China Scholarship Council (CSC file no. 2010646040). J.L. acknowledges financial support from the Defense Threat Reduction Agency (DTRA) under award HDTRA-10-1-0002.

REFERENCES

(1) Cheng, P. H.; Li, D. S.; Li, X. Q.; Liu, T.; Yang, D. R. Localized surface plasmon enhanced photoluminescence from ZnO films: extraction direction and emitting layer thickness. *J. Appl. Phys.* **2009**, *106*, 063120.

(2) Liu, K. W.; Liu, B.; Wang, S. J.; Wei, Z. P.; Wu, T.; Cong, C. X.; Shen, Z. X.; Sun, X. W.; Sun, H. D. Influence of thin metal nanolayers on the photodetective properties of ZnO thin films. *J. Appl. Phys.* **2009**, *106*, 083110.

(3) Ni, W. H.; An, J.; Lai, C. W.; Ong, H. C.; Xu, J. B. Emission enhancement from metallodielectric-capped ZnO films. *J. Appl. Phys.* **2006**, *100*, 026103.

(4) Liu, K. W.; Tang, Y. D.; Cong, C. X.; Sum, T. C.; Huan, A. C. H.; Shen, Z. X.; Wang, Li; Jiang, F. Y.; Sun, X. W.; Sun, H. D. Giant enhancement of top emission from ZnO thin film by nanopatterned Pt. *Appl. Phys. Lett.* **2009**, *94*, 151102.

(5) Lin, H. Y.; Cheng, C. L.; Chou, Y. Y.; Huang, L. L.; Chen, Y. F. Enhancement of band gap emission stimulated by defect loss. *Opt. Exp.* **2006**, *14*, 2372−2379.

(6) Graf, C.; Van Blaaderen, A. Metallodielectric colloidal core−shell particles for photonic applications. *Langmuir* **2002**, *18*, 524−534.

(7) Brown, K. R.; Walter, D. G.; Natan, M. J. Seeding of colloidal Au nanoparticle solutions. 2. Improved control of particle size and shape. *Chem. Mater.* **2000**, *12*, 306−313.

(8) Goia, D. V.; Matijevic, E. Tailoring the particle size of monodispersed colloidal gold. *Colloids Surf., A* **1999**, *146*, 139.

(9) Neeves, A. E.; Birnboim, M. H. Composite structures for the enhancement of nonlinear-optical susceptibility. *J. Opt. Soc. Am.* **1989**, *6*, 787−796.

(10) Oldenburg, S. J.; Averitt, R. D.; Westcott, S. L.; Halas, N. J. Nanoengineering of optical resonances. *Chem. Phys. Lett.* **1998**, *288*, 243−247.

(11) Westcott, S. L.; Oldenburg, S. J.; Lee, T. R.; Halas, N. J. Formation and adsorption of clusters of gold nanoparticles onto functionalized silica nanoparticle surfaces. *Langmuir* **1998**, *14*, 5396−5401.

(12) Stober, W.; Fink, A.; Bohn, E. Controlled growth of monodisperse silica spheres in the micron size range. *J. Colloid Interface Sci.* **1968**, *26*, 62−69.

(13) Vanblaaderen, A.; Vrij, A. Synthesis and Characterization of monodisperse colloidal organo-silica spheres. *J. Colloid Interface Sci.* **1993**, *156*, 1−18.

(14) Waddell, T. G.; Leydenaaa, D. E.; Debello, M. T. The nature of organosilane to silica-surface bonding. *J. Am. Chem. Soc.* **1981**, *103*, 5303−5307.

(15) Duff, D. G.; Baiker, A.; Edwards, P. P. A new hydrosol of gold clusters. 1. Formation and particle size variation. *Langmuir* **1993**, *9*, 2301−2309.

(16) Duff, D. G.; Baiker, A.; Gameson, I.; Edwards, P. P. A new hydrosol of gold clusters. 2. A comparison of some different measurement techniques. *Langmuir* **1993**, *9*, 2310−2317.

(17) Monticone, S.; Tufeu, R.; Kanaev, A. Complex nature of the UV and visible fluorescence of colloidal ZnO nanoparticles. *J. Phys. Chem. B* **1998**, *102*, 2854−2862.

(18) Wu, Y.; Tok, A.; Boey, F.; Zeng, X.; Zhang, X. Surface modification of ZnO nanocrystals. *Appl. Surf. Sci.* **2007**, *253*, 5473−5479.

(19) Wu, L.; Wu, Y.; Pan, X.; Kong, F. Synthesis of ZnO nanorod and the annealing effect on its photoluminescence property. *Opt. Mater.* **2006**, *28*, 418−422.

(20) Cheng, C. W.; Sie, E. J.; Liu, B.; Huan, C. H. A.; Sum, T. C.; Sun, H. D.; Fan, H. J. Surface plasmon enhanced band edge luminescence of ZnO nanorods by capping Au nanoparticles. *Appl. Phys. Lett.* **2010**, *96*, 071107.
(21) Sönnichsen, C.; Franzl, T.; Wilk, T.; Plessen, G.; von; Feldmann, J. Drastic reduction of plasmon damping in gold nanorods. *Phys. Rev. Lett.* **2002**, *88*, 077402.
(22) Lin, H. Y.; Cheng, C. L.; Chou, Y. Y.; Huang, L. L.; Chen, Y. F.; Tsen, K. T. Enhancement of band gap emission stimulated by defect loss. *Opt. Exp.* **2006**, *14*, 2372−2379.
(23) Xiao, X. H.; Ren, F.; Zhou, X. D.; Peng, T. C.; Wu, W.; Peng, X. N.; Yu, X. F.; Jiang, C. Z. Surface plasmon-enhanced light emission using silver nanoparticles embedded in ZnO. *Appl. Phys. Lett.* **2010**, *97*, 071909.